Cusp-condition constraints and the thermodynamic properties of dense hot hydrogen

K. Nagao, S. A. Bonev, and N. W. Ashcroft
Laboratory of Atomic and Solid State Physics, Cornell University, Clark Hall, Ithaca, New York 14853-2501
(Received 27 May 2001; revised manuscript received 6 September 2001; published 26 November 2001)

The thermodynamic properties of liquid hydrogen are investigated at high densities and high temperatures where full molecular dissociation is expected to be attained. Nonlinear electronic response is taken into consideration by imposing rigorous cusp-condition constraints on the electron-nucleus (proton or deuteron) structure factor, and by requiring that it leads to the form of a linear-response theory in the high-density and high-temperature limits. The aim of the new structure factor is to account properly for the accumulation of the electron charge at distances from the nuclei where linear-response theory is insufficient. Using a quasi-one-component model and the Gibbs-Bogoliubov inequality with a hard-sphere reference system, it is shown that, compared with the commonly used linear methods, response with an enforced cusp condition lowers the free energy and leads to a better agreement with recent *ab initio* calculations in the energy and pressure of the hydrogen plasma.

DOI: 10.1103/PhysRevB.64.224111 PACS number(s): 62.50.+p, 52.25.Kn, 05.70.Ce

I. INTRODUCTION

The properties of hydrogen at high densities have been studied extensively[1] over the past several decades, but they still remain unsettled. Part of the motivation for this interest has been the expected molecular dissociation and metallization under the application of external pressure, which was first considered by Wigner and Huntington[2] and is now believed[3] to occur significantly above 300 GPa in the ground state of solid hydrogen. The thermodynamic properties of liquid hydrogen have also been attracting considerable attention in relation to astrophysical problems,[4,5] such as the internal structure and evolution of giant planets (e.g., Jupiter, Saturn, etc.). Recent experiments involving static and dynamic compression techniques[6–10] have already attained pressures in the range of hundreds of gigapascal, and have been uncovering many intriguing features of the dense state of hydrogen. Weir and coworkers[7] have observed a dramatic increase of the conductivity at $\sim$140 GPa and at $\sim$3000 K in a shock-wave experiment, giving evidence of metallization. Other shock-wave experiments[8–10] have produced an unexpected Hugoniot equation of state (EOS), which suggests that hydrogen is more compressible than predicted by the Sesame models.[11] The highest pressures attained by dynamic compression[9] have exceeded 300 GPa at temperatures beyond 30 000 K, where it is presumed that long-lived molecules no longer exist, yet strong correlations between electrons and nuclei (protons or deuterons) still need to be considered.

At the extreme conditions mentioned above, the relevant system can be viewed as a two-component fluid comprised of electrons and nuclei. The electron response and the resulting effective interactions in such two-component problems are frequently dealt with within the linear-response (LR) theory when the ions have closed inner shells. This perturbative approach has been successful in explaining the thermodynamic properties of simple metals, where the interactions between the outer-shell electrons and the ions can be described by weak pseudopotentials. The argument for applying LR to hydrogen, which lacks closed inner shells and is, therefore, characterized by strong electron-nucleus (e-n) interactions, is that nonlinear response is significantly weakened at sufficiently high densities and/or temperatures where the kinetic energy of the electrons is much larger than the screened electrostatic interactions. While such an argument is valid when considering the electronic response in the interstitial region *between* the nuclei, owing to the divergent short-range bare Coulomb potential, LR is insufficient for obtaining the correct e-n correlation in the regions *close* to the nuclei. *Ab initio* molecular dynamics calculations within the local-density approximation is a possible approach to treat the hydrogen liquid beyond LR. However, it is computationally very intensive because the correlation lengths that have to be considered while studying fluids require the use of large supercells, and the computation times are also long if attainment of thermal equilibrium is to be achieved. In addition, the concept of pseudopotentials, which is frequently used even for hydrogen in these *ab initio* calculations, may not be well defined at extreme conditions. Other density-functional-theory methods[12,13] and the quantal hypernetted-chain (QHNC) approximation[14] also give pair-distribution functions valid beyond LR; however, so far they do not lead to a direct access of the free energy and equation of state.

The purpose of this paper is to present a relatively simple analytical method, beyond the LR approximation, for the calculation of both the e-n structure factor and free energy of liquid hydrogen in the high-density and/or high-temperature regime where the molecules are fully dissociated but the e-n correlations remain significant. In the method that we propose, the inhomogeneous electron density is treated in a manner similar to the LR approach, in the sense that it is still considered a superposition of the induced charge density due to the individual nuclei. However, the strength of the e-n correlation is taken into account in a unified way throughout the region of the phase diagram of interest by modifying the Lindhard response function to give the correct cusp behavior of the e-n pair-distribution function. We have achieved this by making use of the cusp condition[15–17] that is a rigorous requirement in systems with singular $-Ze^2/r$ Coulombic in-

teractions, and it relates the charge density to its spherically averaged derivative at $r=0$.

The idea to use the cusp condition to modify the electron response was first proposed by Moulopoulos and Ashcroft[18] (MA), who considered a system with one proton embedded in an interacting electron gas. They obtained a form for the induced charge density, which gives a good improvement over LR at low average densities (e.g., $r_s>1$ for $k_BT \sim 1$ eV). However, at high densities it does not account for the cusp adequately, and even leads to a weaker cusp than LR. We present in this paper an improved form of the electron response, which has the correct high-density cusp behavior. We have also extended the MA formalism to a N_n-nucleus system where the emphasis is shifted from the induced charge density to the e-n structure factor, which is the quantity of major interest in the liquid-state theory.

The derivation of the e-n structure factor is given in Sec. II A. A method for obtaining the free energy of the hydrogen fluid is then described in Sec. II B, where we use a quasi-one-component model[19] and the Gibbs-Bogoliubov inequality (GBI).[19,20] The e-n structure factor, e-n pair-distribution function, and some thermodynamic variables are discussed in Sec. III, where it is shown that our method improves LR and leads to good agreement with results from a recent path-integral Monte-Carlo (PIMC) calculation.[21]

II. METHOD OF CALCULATION

In this section, we consider the general problem of a two-component fluid composed of interacting N_e electrons and N_n nuclei with atomic number Z in a volume V. The mixture is electrically neutral so that $N_e=ZN_n$, and the e-n interactions are treated as pure Coulombic, i.e., without the use of pseudopotentials. The Hamiltonian of the system can be written as a sum of three terms

$$\hat{H}=\hat{H}_n+\hat{H}_e+\hat{V}_{en}, \tag{1}$$

where $\hat{H}_i\equiv\hat{T}_i+\hat{V}_i$ ($i=e$ or n) is the Hamiltonian of the one-component plasma (OCP) consisting of species i, and $\hat{V}_n$, $\hat{V}_e$, and $\hat{V}_{en}$ are given by

$$\hat{V}_n=\frac{1}{2V}{\sum_{\boldsymbol{q}}}' Z^2 v_c(q)[\delta\hat{\rho}_n(-\boldsymbol{q})\delta\hat{\rho}_n(\boldsymbol{q})-N_n], \tag{2}$$

$$\hat{V}_e=\frac{1}{2V}{\sum_{\boldsymbol{q}}}' v_c(q)[\delta\hat{\rho}_e(-\boldsymbol{q})\delta\hat{\rho}_e(\boldsymbol{q})-N_e], \tag{3}$$

$$\hat{V}_{en}=-\frac{1}{V}{\sum_{\boldsymbol{q}}}' Z v_c(q)\delta\hat{\rho}_e(-\boldsymbol{q})\delta\hat{\rho}_n(\boldsymbol{q}). \tag{4}$$

Here, $v_c(q)\equiv 4\pi e^2/q^2$ is the Fourier transform of the e^2/r Coulomb potential, and the primes in the $\boldsymbol{q}$ summations indicate that the $\boldsymbol{q}=0$ terms are excluded. The symbol $\delta\hat{\rho}_i(\boldsymbol{q})$ denotes the Fourier transform of the one-particle-induced density operator of species i,

$$\delta\hat{\rho}_i(\boldsymbol{q})=\int d\boldsymbol{r}\,\exp(-i\boldsymbol{q}\cdot\boldsymbol{r})(\hat{\rho}_i(\boldsymbol{r})-\rho_i), \tag{5}$$

with $\hat{\rho}_i(\boldsymbol{r})$ and ρ_i being the one-particle density operator and the average density, respectively.

In addition, we will assume throughout the paper that the nuclei behave as classical particles, which is a reasonable approximation for the high temperatures of interest ($k_BT>1$ eV). Therefore, the quantum operators $\hat{T}_n$, $\delta\hat{\rho}_n(\boldsymbol{q})$, etc. are hereafter replaced by their corresponding classical quantities T_n, $\delta\rho_n(\boldsymbol{q})$, etc.

A. Cusp-condition constraints on the electron-nucleus structure factor

In principle, the physical properties of a liquid mixture can be described by a set of partial-correlation functions, or partial-structure factors, among its species. In this section, we obtain a form for the e-n structure factor that is an improvement over LR. The e-n structure factor is defined in reciprocal space as[22]

$$S_{en}(q)=\frac{1}{\sqrt{N_eN_n}}\langle\delta\hat{\rho}_e(-\boldsymbol{q})\delta\rho_n(\boldsymbol{q})\rangle. \tag{6}$$

The averaging in Eq. (6) is over both the electron and nuclear degrees of freedom. Having made the assumption that the nuclei obey classical mechanics, the process of averaging can be divided into two steps as follows:

$$S_{en}(q)=\frac{1}{\sqrt{N_eN_n}}\langle\langle\delta\hat{\rho}_e(-\boldsymbol{q})\rangle_e\delta\rho_n(\boldsymbol{q})\rangle_n. \tag{7}$$

In Eq. (7), $\langle\cdots\rangle_e$, and $\langle\cdots\rangle_n$, respectively, indicate averages over the electron states at a fixed nuclear configuration and over the nuclear degrees of freedom, which are explicitly written as

$$\langle\hat{f}_e\rangle_e=\frac{\mathrm{Tr}^{(e)}[e^{-\beta(\hat{H}_e+\hat{V}_{en})}\hat{f}_e]}{\mathrm{Tr}^{(e)}e^{-\beta(\hat{H}_e+\hat{V}_{en})}}, \tag{8}$$

and

$$\langle f_n\rangle_n=\frac{\mathrm{Tr}^{(n)}[e^{-\beta H_n}(\mathrm{Tr}^{(e)}e^{-\beta(\hat{H}_e+\hat{V}_{en})})f_n]}{\mathrm{Tr}^{(n)}[e^{-\beta H_n}(\mathrm{Tr}^{(e)}e^{-\beta(\hat{H}_e+\hat{V}_{en})})]}. \tag{9}$$

Here $\hat{f}_e$ is an operator acting on the electrons, f_n is a classical quantity related to the nuclei, $\mathrm{Tr}^{(e)}$ is a trace over the electron states, and $\mathrm{Tr}^{(n)}$ is a *classical* trace over the nuclear states. Notice that the nuclear configuration enters in the evaluation of $\mathrm{Tr}^{(e)}$ through the e-n interaction $\hat{V}_{en}$. Within the LR approach, $\langle\delta\hat{\rho}_e(-\boldsymbol{q})\rangle_e$ in Eq. (7) is given by

$$\langle\delta\hat{\rho}_e(-\boldsymbol{q})\rangle_e=-\chi^{(1)}(q)Zv_c(q)\delta\rho_n(-\boldsymbol{q}), \tag{10}$$

where $\chi^{(1)}(q)$ is the bare linear-response function of the electron gas. If we employ the local-field correction (LFC) of the homogeneous electron gas (see, for example, Ref. 23) to take account of the exchange-correlation effects, $\chi^{(1)}(q)$ can be expressed as $\chi^{(1)}(q)=\chi_0(q)/(1-v_c(q)\chi_0(q)[1-G(q)])$, where $\chi_0(q)$ is the Lindhard response function of

the ideal (noninteracting) electron gas and $G(q)$ is the LFC. Then, within the LR, the e-n structure factor is

$$S_{en}^{(L)}(q)=\sqrt{\frac{N_n}{N_e}}\frac{Z}{1-G(q)-1/[v_c(q)\chi_0(q)]}S_{nn}(q), \tag{11}$$

where $S_{nn}(q)$ is the nucleus-nucleus (n-n) structure factor defined by

$$S_{nn}(q)=\langle \delta\rho_n(-\boldsymbol{q})\,\delta\rho_n(\boldsymbol{q})\rangle_n/N_n. \tag{12}$$

Let us examine the low-q and high-q limits of Eq. (11), which correspond to long- and short-wavelength disturbances in the electron gas, respectively. In the former case, $\chi_0(q)$ approaches the Thomas-Fermi response function, $\chi_{TF}=-q_0^2/(4\pi e^2)$, where q_0 is the Thomas-Fermi wave number. The low-q behavior of the e-n structure factor from LR is then determined by imposing the rigorous compressibility sum rule[18,24] on the LFC,

$$\lim_{q\to 0}\frac{q_0^2}{q^2}G(q)=1-\frac{K_0}{K}. \tag{13}$$

Here K and K_0 are the isothermal compressibilities of the interacting and noninteracting homogeneous electron gases, namely,

$$K^{-1}=V\left[\frac{\partial}{\partial V}\left(\frac{\partial F_e}{\partial V}\right)_{N_e,T}\right]_{N_e,T}, \tag{14}$$

where F_e (F_{e0}) is the free energy of the interacting (noninteracting) electron gas, for which accurate parametrizations exist.[25–28] Finally, the resulting low-q limit of Eq. (11) is

$$S_{en}^{(L)}(q\to 0)\sim\sqrt{\frac{N_n}{N_e}}\frac{Z}{1+(q^2/q_0^2)(K_0/K)}S_{nn}(q). \tag{15}$$

In the opposite limit of large q, $S_{nn}(q)$ converges to unity, $G(q)$ to a finite constant,[23] and $\chi_0(q)$ behaves as

$$\chi_0(q\to\infty)\sim-\frac{m_e k_F}{\pi^2\hbar^2}\frac{1}{3}\left(\frac{2k_F}{q}\right)^2, \tag{16}$$

where m_e is the electron mass and k_F is the Fermi wave number. Thus, Eq. (11) has the following high-q limit:

$$S_{en}^{(L)}(q\to\infty)\sim\sqrt{\frac{N_n}{N_e}}\,Zv_c(q)\frac{m_e k_F}{\pi^2\hbar^2}\frac{1}{3}\left(\frac{2k_F}{q}\right)^2\propto q^{-4}. \tag{17}$$

It is well known that the LR form (11) does not account correctly for the cusp of the electron density at the nuclear sites, which is closely connected with the high-q values of the e-n structure factor (the high-q behavior is related to the short-range correlations). The correct behavior of $S_{en}(q)$ in the limit of large q is determined by the cusp condition and the corresponding sum rule that must be satisfied by the exact e-n structure factor, namely,[16,17]

$$\sqrt{\rho_e\rho_n}+\frac{1}{(2\pi)^3}\int d\boldsymbol{q}S_{en}(q)=\frac{\hbar^2}{16\pi\mu Ze^2}\lim_{q\to\infty}q^4S_{en}(q), \tag{18}$$

where $\mu\equiv m_e m_n/(m_e+m_n)$ with the nuclear mass m_n.[29] This equation shows that $S_{en}(q)$ must be proportional to q^{-4} at large q, resulting in a cusp in the electron density at the positions of the nuclei. Actually, $S_{en}^{(L)}(q)$ already possesses a q^{-4} proportionality at large q as seen in Eq. (17). However, the coefficient of the q^{-4} term within LR is too small to satisfy Eq. (18), and the resulting cusp is less sharp. This is to be expected from a first-order correction (LR) to the perturbed system, considering that the pure Coulomb potential is singular.

Formally, response beyond linear can be developed in a series of ascending powers of the inducing potentials, namely,

$$\langle\delta\hat{\rho}_e(\boldsymbol{q})\rangle_e=\chi^{(1)}(q)V_{\rm ext}(\boldsymbol{q})+\frac{1}{V}\sum_{\boldsymbol{q}'}\chi^{(2)}(\boldsymbol{q},\boldsymbol{q}')\times V_{\rm ext}(\boldsymbol{q}-\boldsymbol{q}')V_{\rm ext}(\boldsymbol{q}')+\cdots, \tag{19}$$

where $\langle\delta\hat{\rho}_e(\boldsymbol{q})\rangle_e$ is the electron density induced by the unscreened potential $V_{\rm ext}$, and $\chi^{(1)}$, $\chi^{(2)}$, etc. are the linear, quadratic, etc. response functions of the interacting gas. In particular, $\chi^{(2)}$ has been obtained for the noninteracting electron gas at zero temperature by Lloyd and Sholl (and approximations to it at arbitrary degeneracy by Pickenhain, Flietner, and Unger).[30] The complexity of the terms in the series rapidly rises with order and, for an inducing potential of the pure Coulomb type, the first attempt was made by MA to approximately reproduce the entire series [when $V_{\rm ext}$ is a single-impurity potential] through an interpolation, the low-q limit being provided by LR and the high-q limit by the cusp nature of the charge distribution [which we will call the cusp-condition constraints approximation (CCA)]. As one of many possible such interpolations, MA proposed the following form of the electron density for a one-proton system:

$$\langle\delta\hat{\rho}_e(q)\rangle_e=\frac{Z}{1+(q^2/q_0^2)(K_0/K)+q^4/\kappa^4}, \tag{20}$$

where the parameter κ is determined from the cusp condition. The analogous expression for an N_n-nucleus system is then

$$S_{en}(q)=\sqrt{\frac{N_n}{N_e}}\frac{Z}{1+(q^2/q_0^2)(K_0/K)+q^4/\kappa^4}S_{nn}(q) \tag{21}$$

and κ is determined by a direct substitution of Eq. (21) into Eq. (18). As already mentioned in the introduction, this form gives improvement over LR at low densities but not at very high densities. This is because Eq. (21) still places too much weight on the small-q part of $S_{en}^{(L)}(q)$ [i.e., it uses only the small-q part of $S_{en}^{(L)}(q)$]. Hence, we here propose an approximate form for the e-n structure factor, which reproduces the correct high-density limit.

In constructing an interpolation of the e-n structure factor for the CCA, we impose the following restrictions: (i) It is required to include a parameter α $(0 \leqslant \alpha \leqslant 1)$, which is determined from the cusp condition (18), and to exactly reproduce $S_{en}^{(L)}(q)$ when $\alpha = 1$. (ii) It is required to agree with $S_{en}^{(L)}(q)$ at small-q values regardless of α, i.e., to satisfy the compressibility sum rule; (iii) it is required to approach $S_{en}^{(L)}(q)/\alpha$ at large-q values where $S_{en}^{(L)}(q)$ shows appreciable decay. The first restriction is imposed in order to ensure a reasonable limiting behavior at high densities, where the e-n structure factor should approach the LR form. The second and third restrictions serve to remind us that we are concentrating on the nonlinear response related to the cusp, which is principally revealed in the large-q behavior of $S_{en}(q)$. So long as the above restrictions are observed, the physical quantities that depend on the e-n structure factor will be quite insensitive to its exact form. Accordingly, we propose the following interpolation:

$$S_{en}^{(C)}(q) = \sqrt{\frac{N_n}{N_e}} \frac{Z}{1 - G(q) - \dfrac{(1-\alpha)f(q) + \alpha}{v_c(q)\chi_0(q)}} S_{nn}(q), \tag{22}$$

where $f(q) = \chi_0(q)/\chi_0(0)$. This result is simply obtained by making the following replacement in Eq. (11):

$$\chi_0(q) \rightarrow \frac{\chi_0(q)}{(1-\alpha)f(q) + \alpha}, \tag{23}$$

which approaches $\chi_0(q)$ at small q where $f(q) \sim 1$, and $\chi_0(q)/\alpha$ at large q where $f(q) \sim 0$. We should mention here that α, determined from the cusp condition (18), is always less than unity throughout our calculation. Thus, by the replacement (23), the electron response is effectively enhanced at large q, which physically corresponds to further piling up of electron density around each nucleus as is intuitively expected. Again, Eq. (22) can be considered as an approximation to the entire response series concerning the cusp in Eq. (19).

To clarify the physical meaning of the CCA, we can examine $S_{en}^{(C)}(q)$ by replacing $S_{nn}(q)$ in Eq. (22) with a sum of two terms, 1 and $S_{nn}(q) - 1$, corresponding to the one-body and two-body correlations, respectively. It is easy to see then that the corresponding two-body part of the e-n structure factor is little affected by using the CCA instead of its LR form, because $S_{nn}(q) - 1$ converges to zero when $q \rightarrow \infty$. Accordingly, the main effect of the CCA will be restricted to the one-body part. This is to be expected, considering that the CCA deals with the nonlinear response related to the charge accumulation at each nuclear site, and it is basically insensitive to the nuclear configuration. Thus, the CCA can be thought of as a summation of only the one-body parts of all higher-order (beyond linear) response terms.

We can also examine the effect of the CCA by looking at the LFC of the e-n mixture, $G_{ij}(q)$ $(i,j = e$ or $n)$. With their help, the e-n structure factor is exactly written as follows:[28,31]

$$S_{en}(q) = \sqrt{\frac{N_n}{N_e}} \frac{Z(1 - G_{en}(q))}{1 - G_{ee}(q) - 1/(v_c(q)\chi_0(q))} S_{nn}(q). \tag{24}$$

Note that here $G_{ee}(q)$ is not the electron-electron (e-e) LFC of the homogeneous electron gas $G(q)$, but that of the e-n mixture. Substituting Eq. (24) into the cusp condition (18), we find that

$$G_{en}(q \rightarrow \infty) = 1 - g_{en}(0), \tag{25}$$

where $g_{en}(r)$ is the e-n pair-distribution function; the pair-distribution functions are generally related to the structure factors as follows:

$$g_{ij}(r) = 1 + \frac{1}{\sqrt{\rho_i \rho_j}} \int \frac{d\boldsymbol{q}}{(2\pi)^3} [S_{ij}(q) - \delta_{i,j}] \exp(-i\boldsymbol{q} \cdot \boldsymbol{r}). \tag{26}$$

Since $g_{en}(0)$ is larger than unity, $G_{en}(q)$ must tend toward a negative value at high q.[32,33] However, comparing the LR structure factor (11) with Eq. (24), we find that $G_{en}(q) = 0$ and $G_{ee}(q) = G(q)$ within LR. This contradicts the negative property of $G_{en}(q)$ required from Eq. (25), which is another way to see the violation of the cusp condition within LR. In the case of the CCA, on the other hand, by comparing Eq. (22) with Eq. (24) together with the jellium approximation $G_{ee}(q) = G(q)$, the e-n LFC is written as

$$G_{en}(q) = \frac{(1-\alpha)f(q) + \alpha - 1}{(1-\alpha)f(q) + \alpha - v_c(q)\chi_0(q)[1 - G(q)]}. \tag{27}$$

The high-q behavior is now, $G_{en}(q \rightarrow \infty) = 1 - 1/\alpha$, and since α is always less than unity as already stated, the CCA satisfies the negative property of $G_{en}(q)$ at large q.

B. Quasi-one-component model and Gibbs-Bogoliubov inequality

Having obtained $S_{en}(q)$, we can now use the standard quasi-one-component model and the GBI to obtain the Helmholtz free energy F as a function of density and temperature, from which almost all thermodynamic quantities of the liquid mixture can be derived. For a system where the nuclei are treated as classical particles, it is possible to reduce the electron-nucleus two-component problem to a quasi-one-component problem.[19] In this approach, we only need to deal with a system composed of nuclei, having total effective interaction energy

$$V_{eff} = V_n + F_e + U_n, \tag{28}$$

where F_e and U_n are given by

$$F_e = -k_B T \ln \mathrm{Tr}^{(e)} e^{-\beta \hat{H}_e}, \tag{29}$$

and

$$U_n = \int_0^1 d\lambda \langle \hat{V}_{en} \rangle_{e(\lambda)}. \tag{30}$$

Here F_e is the free energy of a uniform interacting electron gas for which convenient parametrizations exist in the literature as already mentioned in Sec. II A.[25–28] The definition of $\langle\cdots\rangle_{e(\lambda)}$ in Eq. (30) is identical to that in Eq. (8), but with $\hat{V}_{en}$ replaced by $\lambda\hat{V}_{en}$, where the quantity λ is a coupling-constant parameter introduced as a scaling factor in the e-n interaction. The expression of the effective potential in Eq. (28) is exact so long as the nuclei can be considered classical particles, but it is only a formal relation because U_n is still unknown.

For the estimation of the total free energy F, we exploit the GBI that is a rigorous theorem in classical systems, namely,

$$F \leqslant F_r + \langle V_{eff} - V_r \rangle_r , \tag{31}$$

where F_r and V_r are the free energy and the potential of a reference system, and the average $\langle\cdots\rangle_r$ is taken by using the distribution function of the reference system. When the temperature is high enough to overcome the n-n screened interaction around the mean nearest-neighbor distance, the structure of the liquid will be determined mostly by the repulsive core part of the interaction and will be insensitive to its detailed shape. Therefore, under such conditions, we can apply the GBI with a hard-sphere (HS) reference system, and regard the packing fraction η as a variational parameter (the use of a HS system as an appropriate reference system is further examined in Sec. III). By substituting Eq. (28) into Eq. (31) and considering that the free energy of the HS system is entirely entropic, we can rewrite the GBI as[19]

$$F \leqslant F_{gas} - T\Delta s(\eta) + F_e + \langle V_n \rangle_{n(\eta)} + \langle U_n \rangle_{n(\eta)} , \tag{32}$$

where F_{gas} is the free energy of the ideal gas consisting of nuclei, and $\Delta s(\eta)$ is the excess entropy of the HS system. The bracket $\langle\cdots\rangle_{n(\eta)}$ indicates an average over nuclear configurations taken by the distribution function of the HS system with a packing fraction η. Here, we invoke the Percus-Yevick (PY) approximation, which is known to be a good approximation for a HS system and, moreover, has an analytic solution.[34] Then, $\Delta s(\eta)$ can be written using the empirical but accurate expression of Carnahan and Starling,[19,35]

$$\Delta s(\eta) = -N_n k_B \eta \frac{4-3\eta}{(1-\eta)^2} . \tag{33}$$

Also, we can use the analytic form for the Madelung energy $\langle V_n \rangle_{n(\eta)}$ given by Jones,[19,36]

$$\langle V_n \rangle_{n(\eta)} = N_n \frac{2Z^2}{Z^{1/3} r_s} (-3\eta^{2/3}) \frac{1 - \eta/5 + \eta^2/10}{1+2\eta} \mathrm{Ry}, \tag{34}$$

where r_s is defined by $4\pi(r_s a_0)^3/3 = V/N_e$.

The quantity $\langle U_n \rangle_{n(\eta)}$ in Eq. (32) is directly related to a (λ-dependent) e-n structure factor. After rewriting $\langle U_n \rangle_{n(\eta)}$ using Eqs. (4) and (30), we find the connection between $\langle U_n \rangle_{n(\eta)}$ and the e-n structure factor as follows:

$$\begin{aligned}\langle U_n \rangle_{n(\eta)} &= -\frac{\sqrt{N_e N_n}}{V} {\sum_{\boldsymbol{q}}}' Z v_c(q) \int_0^1 d\lambda S_{en}(q,\lambda;\eta) \\ &= -\sqrt{N_e N_n} \frac{1}{2\pi^2} \int_0^\infty dq q^2 Z v_c(q) \\ &\quad \times \int_0^1 d\lambda S_{en}(q,\lambda;\eta),\end{aligned} \tag{35}$$

where

$$S_{en}(q,\lambda;\eta) \equiv \frac{1}{\sqrt{N_e N_n}} \langle\langle \delta\hat{\rho}_e(-\boldsymbol{q}) \rangle_{e(\lambda)} \delta\rho_n(\boldsymbol{q}) \rangle_{n(\eta)} . \tag{36}$$

This e-n structure factor can be calculated using Eq. (11) (LR) or Eq. (22) (CCA), where we use the n-n structure factor obtained by the PY approximation, namely, $S_{nn}(q;\eta) \sim 1/\{1-\rho_n c^{PY}(q\sigma)\}$; here σ is the diameter of the HS, $\sigma = 2Z^{1/3} r_s a_0 \eta^{1/3}$, and $c^{PY}(y)$ is the Fourier transform of the Ornstein-Zernike function, i.e.,

$$\begin{aligned}c^{PY}(y) = -4\pi\sigma^3 \Bigg[&\frac{24C}{y^6} - \frac{2B}{y^4} + \sin(y) \left\{ \frac{A+2B+4C}{y^3} - \frac{24C}{y^5} \right\} \\ &+ \cos(y) \left\{ -\frac{A+B+C}{y^2} + \frac{2B+12C}{y^4} - \frac{24C}{y^6} \right\} \Bigg],\end{aligned} \tag{37}$$

with $A = (1+2\eta)^2/(1-\eta)^4$, $B = -6\eta(1+\eta/2)^2/(1-\eta)^4$, $C = \eta A/2$.[34] We should note here that the coupling constant λ is explicitly included in Eq. (36). Therefore, when we use the methods presented in Sec. II A, we need to replace Z with λZ in Eqs. (11), (18), and (22). This also means that, in the CCA, the parameter α must be determined separately for each λ. Then, we can evaluate $\langle U_n \rangle_{n(\eta)}$ by carrying out the numerical integrations[37] with respect to q and λ in Eq. (35). At this point, all terms appearing in the GBI are known, and the free energy can, therefore, be obtained by minimizing the right-hand side of Eq. (32) with respect to η.

III. RESULTS

All calculations in this section are carried out for deuterium[38] to compare our results with recent experiments[8,9] and also with other *ab initio* calculations.[21,39,40] In order to apply the method presented in Sec. II, we need to specify F_e, $\chi_0(q)$, and $G(q)$. Here, we use the parametrizations of F_e and $\chi_0(q)$ given by Dandrea, Ashcroft, and Carlsson,[27] and $G(q)$ provided by Vashishta and Singwi,[41] namely, $G(q) = a(1-\exp[-bq^2])$, where the parameters a and b are fully determined from the cusp condition [$G(q \to \infty) = 1 - g_{ee}(0)$] (Refs. 23 and 42) and the compressibility sum rule[18,24] for the homogeneous electron gas.

The e-n structure factor at $\lambda = 1$ is plotted in Fig. 1 for $\Gamma = 1$, where Γ is the Coulomb coupling parameter defined

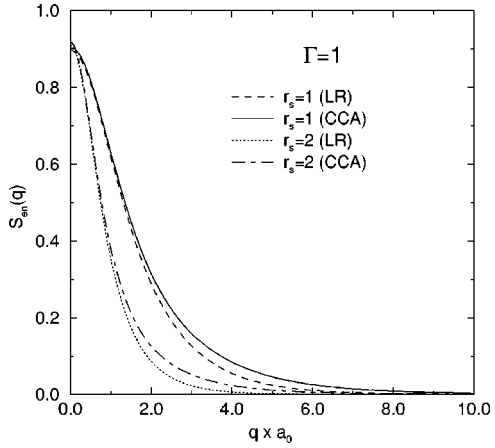

FIG. 1. Electron-nucleus structure factor $S_{en}(q)$; a comparison between the CCA and LR results (see text).

by $\Gamma \equiv e^2/(r_s a_0 k_B T)$. The figure clearly shows that the CCA significantly enhances $S_{en}(q)$ at large q compared with the LR result. The difference diminishes at small q, but remains finite even at $q=0$ because the packing fraction η is different in the two cases; recall that η is a variational parameter in expression (32), and, therefore, it depends on the method used to obtain $\langle U_n \rangle_{n(\eta)}$. It is intuitively apparent that the CCA must lead to a smaller packing fraction than LR because it provides for better screening of the nuclei. A smaller η then yields larger $S_{nn}(q=0)$ and $S_{en}(q=0)$.

The effect of enhanced $S_{en}(q)$ at high q seen within the CCA must be observed in real space as a larger charge accumulation at the sites of the nuclei. To ascertain this, we have calculated the e-n pair-distribution function $g_{en}(r)$ through the Fourier transform (26). The results are shown in Fig. 2 and, as expected, the CCA dramatically heightens the cusp around the origin compared with LR. Because the CCA represents an improvement over LR related to the one-body part of the nuclear correlation, its major effect, which is more prominent at lower densities, is confined to a sphere of radius $r=a_0 r_s$ about each nucleus.

In order to investigate the improvement of the CCA on the

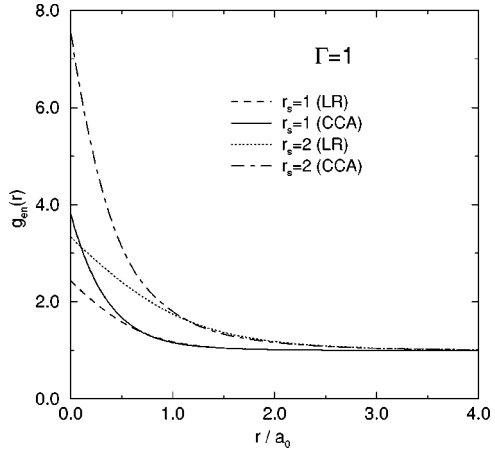

FIG. 2. Electron-nucleus pair-distribution function $g_{en}(r)$ within the CCA and LR.

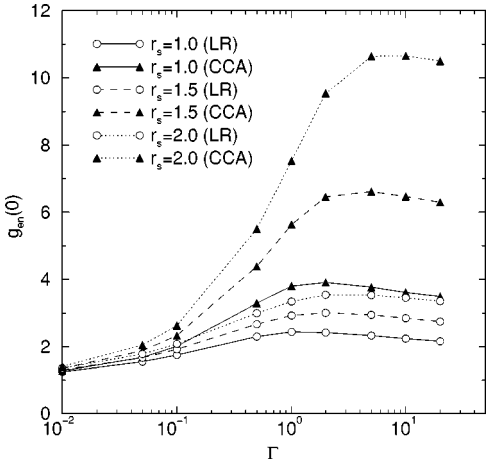

FIG. 3. Electron-nucleus pair-distribution function at the origin $g_{en}(0)$ as a function of the Coulomb coupling parameter Γ and at various values of the density parameter r_s.

cusp at various densities and temperatures, we have calculated and plotted $g_{en}(0)$ (a measure of the cusp) in Fig. 3 as a function of Γ for various r_s values. The CCA always gives a larger $g_{en}(0)$ compared to LR under the conditions studied here, and the difference between them lessens as Γ or r_s is decreased, which confirms that the CCA has the correct high-density and high-temperature limits. It is intriguing to note that within both LR and CCA, $g_{en}(0)$ has different Γ dependences at small- and large-Γ values; while it is monotonously increasing in the former, it is decreasing in the latter case. This behavior was previously pointed out by Dharmawardana and Perrot[12] and also by Chihara,[14] and the reason behind it is the different temperature dependences of the quantities $\chi_0(q)$ and $S_{nn}(q)$, which enter the calculation of $g_{en}(r)$. At a small value of the Coulomb coupling parameter, where the electron system is nondegenerate, the temperature dependence of $\chi_0(q)$ is dominant because the absolute value of $\chi_0(q)$ grows appreciably upon increase of Γ and the ''turning on'' of the quantum degeneracy. On the other hand, $\chi_0(q)$ is not so sensitive to the temperature at large Γ because the electron system there is already strongly degenerate. However, in this regime, the nuclei are highly coupled with one another and their mutual screening is driven by correlation and the associated repulsion from other nuclei, so $S_{nn}(q)$ remains temperature sensitive, and this leads to the observed slight negative slope of $g_{en}(0)$.

Next, we examine $G_{en}(q)$, which is obtained as one of the outcomes of the CCA through Eq. (27) and is useful to capture the physical meanings of it in connection with the other treatments. Figure 4 exhibits the $G_{en}(q)$, and we notice that it is always negative. This behavior was previously observed in QHNC calculations by Chihara,[32] where the nonlinear response is sufficiently included by directly solving a one-electron Schrödinger equation in a self-consistent potential. Further, Tanaka, Yan, and Ichimaru[33] pointed out a similar tendency in $G_{en}(q)$ by using a modified convolution approximation, taking account of the strong electron-nucleus correlation. This negative property of $G_{en}(q)$ implies an effective attraction between electrons and nuclei in addition to

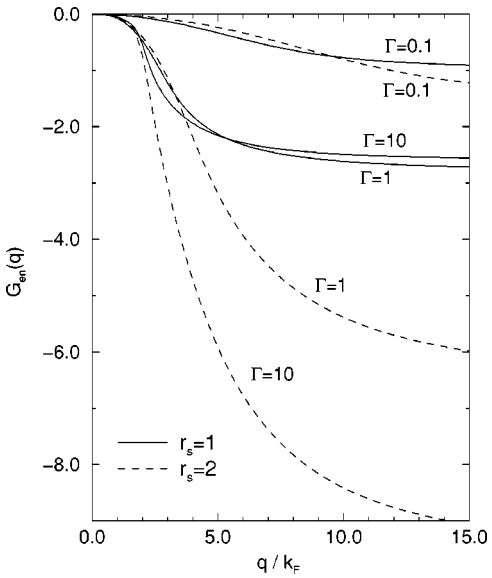

FIG. 4. Electron-nucleus local field correction $G_{en}(q)$ within the CCA.

the bare Coulomb interaction. Note that, at $r_s=1$, the curve of $\Gamma=10$ shows smaller absolute values at high value of q than observed at $\Gamma=1$, while it is not the case at $r_s=2$. This can be interpreted in terms of $g_{en}(0)$ through the relation (25); as shown in Fig. 3, $g_{en}(0)$ at $r_s=1$ has a slightly larger value at $\Gamma=1$ than at $\Gamma=10$.

The enhanced cusp observed within the CCA is related to a stronger e-n coupling than in LR, and it is expected to lower the free energy F. To elucidate this point, we now investigate the e-n coupling part of the free energy defined by $\Delta F=F-F_e-F_n$, where F_n is the free energy of a nuclear OCP given by $F_n=-k_BT\ln \mathrm{Tr}^{(n)}\exp(-\beta H_n)$. Here F_n can be written as a sum of an ideal gas and an excess free-energy part, namely, $F_n=F_{gas}+F_{ex}$, and the latter can be calculated from the relation

$$\beta F_{ex}=\int_0^{\Gamma}\frac{d\Gamma'}{\Gamma'}u_{ex}(\Gamma'), \tag{38}$$

where $u_{ex}(\Gamma)\equiv\beta E_{ex}$ with E_{ex} being the excess energy. Accurate estimates for $u_{ex}(\Gamma)$ have been obtained by the cluster expansion method[43] for $\Gamma<0.1$, by the HNC approximation for $0.1<\Gamma<1$, and from a Monte Carlo simulation[44] for $1<\Gamma$. The resulting ΔF is shown in Fig. 5 as a function of r_s for some fixed temperatures. As anticipated, the CCA lowers the free energy compared to the LR. Also, the results show again that the CCA has the correct high-density limit, where it approaches LR. It is interesting to note that the CCA results approach those of LR at low densities as well when the temperature is high, as is evident from the $T=10^5$ K data in Fig. 5. This is related to the degree of degeneracy of the electron system; at low density, where the Fermi temperature is also low, the electron response is easily suppressed by temperature effects, which leads to the decrease of the difference between LR and CCA.

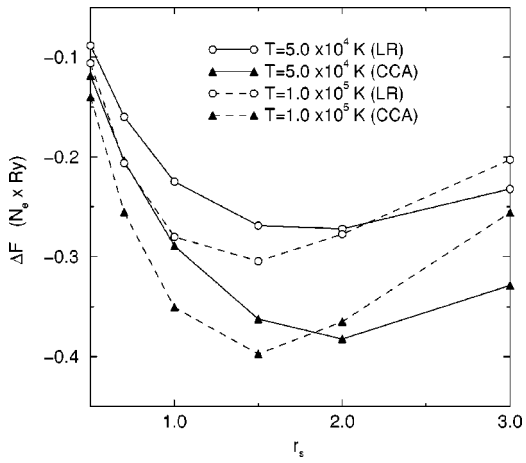

FIG. 5. Electron-nucleus coupling part of free energy, $\Delta F=F-F_e-F_n$, as a function of r_s; here F_e is the free energy of an interacting homogeneous electron gas and F_n is that of a nuclear (classical) OCP.

We should point out that ΔF continues to increase rapidly at small r_s. This unphysical behavior takes place because the HS system used here simply becomes a less satisfactory reference system for the GBI at densities so high that the long-range character of the interactions between the nuclei is prominent. To establish quantitatively the conditions at which the use of HS is adequate, we therefore examine the screened Coulomb coupling parameter, $\Gamma^*=\Gamma\exp(-q_0r_sa_0)$, which is the ratio of the Yukawa interaction around the mean distance of the nearest-neighbor nuclei to the temperature k_BT. When Γ^* is small, the core repulsive part of the potential between nuclei plays a dominant role in determining the structure of the liquid, and the hard spheres will be a fairly good reference system. Figure 6 shows contour lines of Γ^* in the r_s-T plane that is divided into two parts (one of them shaded) by the contour of $\Gamma^*=1$. The

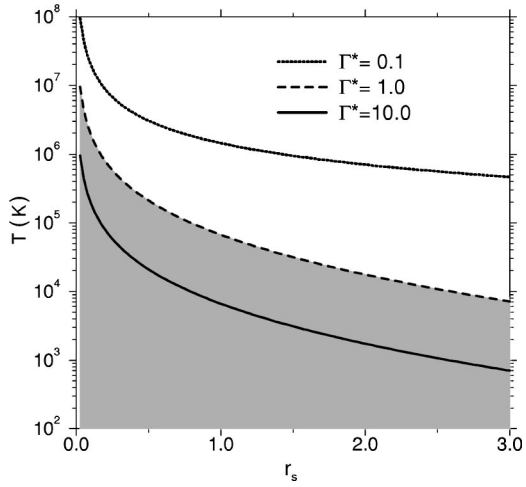

FIG. 6. Screened-Coulomb coupling parameter Γ^* in the (r_s-T) plane. Γ^* is defined by $\Gamma^*\equiv\Gamma\exp(-q_0r_sa_0)$, where q_0 is the Thomas-Fermi wave number. The shaded region marks the area where the long-range character of the interaction among the nuclei is significant.

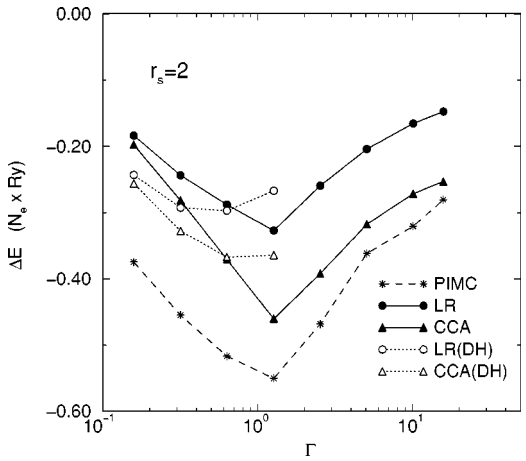

FIG. 7. Γ dependence of the coupling part of the energy, $\Delta E = E - E_e - E_n$, at $r_s = 2$. The path-integral Monte Carlo results are from Ref. 21 and data labeled DH are from calculations with the nucleus-nucleus structure factor obtained by applying the Debye-Hückel approximation to a linearly screened nuclear system (see the Appendix).

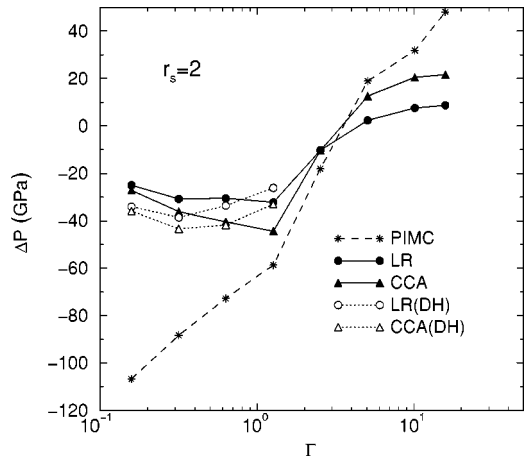

FIG. 8. Γ dependence of the coupling part of pressure, $\Delta P = P - P_e - P_n$, in comparison with the path-integral Monte Carlo results[21] at $r_s = 2$.

shaded region is roughly the area where the HS is a less-suitable reference. For example, the boundary of the two areas at $T = 10^5$ K is located at $r_s \sim 0.77$, and at higher density the HS reference is likely to be less accurate. However, note that even in this region it is still meaningful to use the HS model if the aim is to examine the possible improvement of the CCA over the LR.

We also compare the energy and pressure obtained by the method presented here with those from PIMC.[21] The PIMC method treats both electrons and nuclei as quantum particles even beyond the adiabatic approximation, and it is considered a very reliable approach even though it employs the fixed-node approximation and supercells of finite sizes. Figure 7 displays the corresponding *e-n* coupling part of the energy, $\Delta E = E - E_e - E_n$, as a function of Γ at $r_s = 2$. At large Γ, the CCA is in good agreement with the PIMC, and its improvement over LR is significant; for example, the energy difference between LR and CCA at $\Gamma = 15.8$ corresponds to ~10% of the absolute value of the total energy. However, the CCA energy curve gradually deviates from the PIMC as Γ is reduced and the deviation becomes appreciable for $\Gamma < 1$, though the differences still remain very small compared to the total energy. This observation may raise a question about the validity of the HS reference at small Γ. Figure 6 already summarizes the conditions at which the HS reference is appropriate, using the criterion $\Gamma^* < 1$, which is reasonable but somewhat intuitive as well. According to this criterion, the HS system seems to be a suitable reference at small Γ; nevertheless, to establish its validity more firmly, we have carried out an alternative calculation (see the Appendix) and estimated the errors resulting from the use of the HS system. In this calculation, for obtaining the *n-n* structure factor, we have applied the Debye-Hückel (DH) method to a linearly screened nuclear system, which is a satisfactory approximation in a weakly coupled regime (small-Γ^* region). The free energy is then calculated directly from a coupling-constant integration without the use of the GBI since the *n-n* structure factor can be easily determined at each λ from the DH approximation. The results obtained by the method are also shown in Fig. 7, which are labeled as LR (DH) and CCA (DH). We have found that the use of the DH method gives energies close to those of the HS model at small Γ, and this confirms that the latter remains a suitable reference system in this range.

Figure 8 shows the corresponding *e-n* coupling part of the pressure, $\Delta P = P - P_e - P_n$. The CCA again improves the LR results and always works to reduce the discrepancy with the PIMC. Both LR and CCA give lower ΔP than PIMC at large Γ, and this can be attributed to the fact that these methods do not take account of the possible pairing of nuclei, since it has been suggested[39,45] that a small concentration of molecules (with a short lifetime) still exists at $\Gamma \sim 15$ and at $r_s = 2$. Notice that, at large Γ, the CCA energy in Fig. 7 is in better agreement with the PIMC than is the pressure (despite the neglect of the nuclear pairing there as well). This indicates that the pressure, which is obtained from the derivative of the free energy with respect to the volume, is a more sensitive test for comparison than the energy. At higher temperatures (around $1 < \Gamma < 10$) where no nuclei are expected to be paired, the CCA and PIMC agree quite well. But as in the case of the energy, our results differ from the PIMC at small Γ, and this is independent of the choice of a reference system (HS or DH). At these high temperatures, however, the discrepancies are considered small compared to the total pressure: At $\Gamma = 0.158$, for example, the difference corresponds to only ~1.5% of the total pressure.

Lastly, we discuss the Hugoniot EOS of deuterium where, as we will show, the importance of the nonlinear response is even more clearly observed. The Hugoniot EOS is determined by $E - E_0 = (P + P_0)(V_0 - V)/2$, where E_0, P_0, and V_0 are the initial energy, pressure, and volume, respectively, and the locus of final states, *E*, *P*, and *V*, constitutes the Hugoniot curve. Many theoretical attempts have been made to account for the remarkable Hugoniot EOS observed in recent shock experiments.[8,9] So far, the linear mixing model[46] and the chemical model[5] have provided rather good agreements, while *ab initio* calculations[21,40] have shown

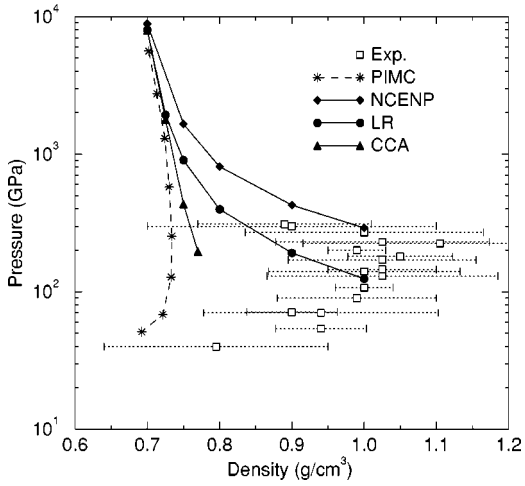

FIG. 9. Hugoniot equation of state of deuterium. Experimental results (Exp.) are from Refs. 8 and 9, and the path-integral Monte Carlo results are from Ref. 21. The Hugoniot of a noncoupled electron-nucleus plasma, with electron-nucleus interaction $\hat{V}_{en}$ set to zero, is also shown.

large discrepancies with the experiments. The reason for this difference is still a matter of active debate.

Our Hugoniot EOS, together with experimental[8,9] and PIMC[21] results, is shown in Fig. 9. We find that the CCA agrees very well with the PIMC and hence leads to a significant deviation from experiments. As the pressure is decreased, the CCA Hugoniot also gradually deviates from the PIMC, and the difference becomes perceivable around 200 GPa, although it is still small compared to the difference from the experiments. It is likely that this deviation of the CCA from the PIMC at low pressure may again be related to the circumstances that the CCA does not deal with the pairing of the nuclei.

As noted above, we have invoked an adiabatic separation of electronic and nuclear time scales; deviations from adiabatic adjustment are gauged by the parameter $(m_e/m_n)^{1/4}$ and this is small. When the band gap declines to the vibron energy ($\hbar\omega_v$), there can be mixing of states and a pathway opens for the transfer of energy from the nuclear to the electronic system. However, as the gap declines further, nonadiabatic excitation should again diminish. Given this, the present results, as with other treatments, remain in some conflict with experiments.

In Fig. 9, we also show the Hugoniots from LR and from a noncoupled e-n plasma (NCENP) model where the e-n interaction is set to zero. The comparison between the NCENP, LR, and the CCA shows that a better evaluation of the e-n coupling tends to shift the Hugoniot curve to the low-density region. The fact that LR exhibits a behavior more similar to the NCENP than to the CCA at low pressure (around 200 GPa) implies that the Hugoniot is very sensitive to the treatment of the e-n coupling, and it is, therefore, essential to deal with the electronic response beyond the LR approximation.

IV. SUMMARY AND CONCLUSIONS

In summary, we have proposed an interpolation form for the e-n structure factor that has a correct limiting behavior at high densities, and it can be used for calculations of the free energy of dense liquid hydrogen beyond LR. The CCA method presented here is a modification and an extension to N_n-nucleus systems of the idea of MA (Ref. 18) for an improvement over LR by enforcement of the rigorous cusp condition on the electronic response. The cusp-condition constraint requires $G_{en}(q)$ to take on negative values in accordance with previous results,[32,33] suggesting the presence of an additional attractive e-n correlation (which is constrained to zero within LR). Compared to LR, the CCA therefore leads to a dramatic enhancement of the $g_{en}(r)$ cusp, which correspondingly lowers the free energy and also leads to a better agreement with PIMC in both energy and pressure. In addition, we have found that the Hugoniot EOS is reasonably sensitive to the treatment of the electron response.

The GBI combined with a HS reference system works well at low densities where the screening lengths are sufficiently smaller than $r_s a_0$; however, at extremely high densities, a more sophisticated reference system is needed. The CCA only accounts for the nonlinear response around the positions of nuclei, and, therefore, it is suitable for the *atomic* phase. A complete nonlinear response in the interstitial region (ultimately represented as a covalent bond) is beyond the scope of this paper; it would require at least the consideration of higher-order two-body parts in e-n structure factor together with the one-body part obtained by CCA.

The CCA is potentially applicable to elements other than hydrogen. One conceivable choice is helium, where no inner shells exist and the cusp condition is satisfied for the structure factor. Even for other light elements that have inner shells, the CCA may again be useful. For example, in a plasma at extremely high densities or temperatures, the classification of core and valence electrons becomes imprecise and, consequently, pseudopotentials are not well defined there. Under such conditions, it is necessary to treat the core and valence electrons on the same footing and in a context where they interact with the nuclei through a divergent Coulomb potential, and, therefore, the inclusion of the nonlinear response is indispensable.

ACKNOWLEDGMENTS

This work was supported by the National Science Foundation under Grant No. DMR-9988576. K.N. was supported by the Japan Society for the Promotion of Science from 1999 through 2001.

APPENDIX

We present here an alternative method to the approach discussed in Sec. II B for obtaining the free energy. In the following, we again introduce a coupling constant λ to the e-n interaction part $\hat{V}_{en}$ and define the free energy at given λ as

$$F(\lambda) = -k_B T \ln \mathrm{Tr}\, \exp[-\beta(\hat{H}_n + \hat{H}_e + \lambda \hat{V}_{en})]. \quad \text{(A1)}$$

The derivative of $F(\lambda)$ with respect to λ then yields

$$\frac{dF(\lambda)}{d\lambda}=\langle \hat{V}_{en}\rangle_\lambda , \tag{A2}$$

where the average $\langle\cdots\rangle_\lambda$ is defined by

$$\langle \hat{f}\rangle_\lambda \equiv \frac{\mathrm{Tr}\ \exp[-\beta(\hat{H}_n+\hat{H}_e+\lambda\hat{V}_{en})]\hat{f}}{\mathrm{Tr}\ \exp[-\beta(\hat{H}_n+\hat{H}_e+\lambda\hat{V}_{en})]}. \tag{A3}$$

Assuming that there is no phase change when λ varies between zero and 1, we can integrate Eq. (A2) to obtain

$$F=F_e+F_n+\int_0^1 d\lambda\langle \hat{V}_{en}\rangle_\lambda . \tag{A4}$$

Here, $F=F(\lambda=1)$ is the actual free energy, and F_e and F_n are the free energies of the interacting electron gas[25–28] and the nuclear OCP,[43,44] respectively. The last term in Eq. (A4) represents the e-n coupling part of the free energy and can be rewritten as

$$\begin{aligned}\int_0^1 d\lambda\langle \hat{V}_{en}\rangle_\lambda &= -\frac{\sqrt{N_nN_e}}{V}{\sum_{\boldsymbol{q}}}' Zv_c(q)\int_0^1 d\lambda S_{en}(q,\lambda),\\ &= -\sqrt{N_nN_e}\frac{1}{2\pi^2}\int_0^1 dq q^2 Zv_c(q)\\ &\quad\times\int_0^1 d\lambda S_{en}(q,\lambda),\end{aligned} \tag{A5}$$

where we have used Eq. (4) together with the definition of the e-n structure factor

$$S_{en}(q,\lambda)=\frac{1}{\sqrt{N_nN_e}}\langle \delta\hat{\rho}_e(-\boldsymbol{q})\delta\hat{\rho}_n(\boldsymbol{q})\rangle_\lambda . \tag{A6}$$

Now, assuming that the nuclei are classical particles, the e-n structure factor becomes

$$S_{en}(q,\lambda)\sim\frac{1}{\sqrt{N_nN_e}}\langle\langle \delta\hat{\rho}_e(-\boldsymbol{q})\rangle_{e(\lambda)}\delta\rho_n(\boldsymbol{q})\rangle_{n(\lambda)}, \tag{A7}$$

where the definitions of $\langle\cdots\rangle_{e(\lambda)}$ and $\langle\cdots\rangle_{n(\lambda)}$ are obtained from Eqs. (8) and (9) with the replacement of $\hat{V}_{en}$ by $\lambda\hat{V}_{en}$. For the calculation of $S_{en}(q,\lambda)$, we can use either LR or the CCA, which are discussed in Sec. II A. At this point, we should emphasize that the average over the nuclear states in Eq. (A7) depends on λ, which means that we need to make the replacement $S_{nn}(q)\rightarrow S_{nn}(q,\lambda)$ together with $Z\rightarrow\lambda Z$ in both Eq. (11) and Eq. (22). Furthermore, this approach requires knowledge of the n-n structure factor in advance, since it directly calculates the free energy; this is a major difference from GBI discussed in Sec. II B where the n-n structure factor is determined through minimization of Eq. (32) and the resulting free energy is an upper bound of the real one.

Here we employ a simple method to obtain $S_{nn}(q,\lambda)$, which uses the Debye-Hückel approach to a linearly screened nuclear system and is, therefore, valid only at small Γ^*. Consider an assembly of nuclei and electrons with a given nucleus fixed at the origin and with a scaled e-n interaction λV_{en}. The averaged densities of the electrons and the nuclei in this *inhomogeneous* system, $\langle\rho_i(r,\lambda|n)\rangle$ ($i=e$ or n), are related to the pair-distribution functions of the *homogeneous* system, $g_{in}(r,\lambda)$, by the following relation:[31]

$$\langle\delta\rho_i(r,\lambda|n)\rangle=\rho_i[g_{in}(r,\lambda)-1], \tag{A8}$$

where $\langle\delta\rho_i(r,\lambda|n)\rangle\equiv\langle\rho_i(r,\lambda|n)\rangle-\rho_i$. In reciprocal space, this becomes

$$\langle\delta\rho_i(q,\lambda|n)\rangle=\sqrt{\frac{\rho_i}{\rho_n}}[S_{in}(q,\lambda)-\delta_{i,n}], \tag{A9}$$

where we have used the relation (26). Hence, to evaluate the n-n structure factor of the *homogeneous* system, we first derive the expression of $\langle\delta\rho_n(q,\lambda|n)\rangle$ for the *inhomogeneous* system. Then, through relation (A9), we can obtain the n-n structure factor.

In the system with a nucleus fixed at origin, the electric potential acting on the nuclei, $\phi_n(r,\lambda|n)$, satisfies the following Poisson equation:

$$\begin{aligned}\triangle\phi_n(r,\lambda|n)=&-4\pi[(Ze)^2\{\langle\delta\rho_n(r,\lambda|n)\rangle+\delta(r)\}\\ &-\lambda Ze^2\langle\delta\rho_e(r,\lambda|n)\rangle].\end{aligned} \tag{A10}$$

The Fourier transform of this equation yields

$$\begin{aligned}-q^2\phi_n(q,\lambda|n)&=-4\pi[(Ze)^2\{\langle\delta\rho_n(q,\lambda|n)\rangle+1\}\\ &\quad-\lambda Ze^2\langle\delta\rho_e(q,\lambda|n)\rangle]\\ &=-4\pi(Ze)^2\{1+\lambda^2v_c(q)\chi^{(1)}(q)\}\\ &\quad\times\{\langle\delta\rho_n(q,\lambda|n)\rangle+1\},\end{aligned} \tag{A11}$$

where, in the second equation, we have used the linear-response relation

$$\langle\delta\rho_e(q,\lambda|n)\rangle=\chi^{(1)}(q)\{-\lambda Zv_c(q)\}\{\langle\delta\rho_n(q,\lambda|n)\rangle+1\}, \tag{A12}$$

with the bare response function $\chi^{(1)}(q)=\chi_0(q)/(1-v_c(q)\chi_0(q)[1-G(q)])$. Here, as in Sec. III, we use the Dandrea, Ashcroft, and Carlsson fitting for $\chi_0(q)$ (Ref. 27) and the Vashishta-Singwi form for $G(q)$.[41] On the other hand, assuming a Boltzmann distribution for nuclei, we have another relation between $\langle\rho_n(r,\lambda|n)\rangle$ and $\phi_n(r,\lambda|n)$, namely,

$$\langle\rho_n(r,\lambda|n)\rangle=\rho_n\exp[-\beta\phi_n(r,\lambda|n)]\sim\rho_n[1-\beta\phi_n(r,\lambda|n)], \tag{A13}$$

where we have linearized $\langle\rho_n(r,\lambda|n)\rangle$ with respect to $\phi_n(r,\lambda|n)$. Then, in reciprocal space,

$$\langle\delta\rho_n(q,\lambda|n)\rangle=-\rho_n\beta\phi_n(q,\lambda|n). \tag{A14}$$

The combination of Eqs. (A11) and (A14) yields

$$\langle \delta\rho_n(q,\lambda|n)\rangle = \frac{-q_D^2}{\epsilon(q,\lambda)q^2+q_D^2}, \tag{A15}$$

where

$$q_D \equiv 4\pi(Ze)^2\rho_n\beta, \tag{A16}$$

$$\epsilon(q,\lambda) \equiv 1/\{1+\lambda^2 v_c(q)\chi^{(1)}(q)\}. \tag{A17}$$

Finally, from Eqs. (A9) and (A15), the n-n structure factor is expressed as follows:

$$S_{nn}(q,\lambda) = \frac{\epsilon(q,\lambda)q^2}{\epsilon(q,\lambda)q^2+q_D^2}. \tag{A18}$$

Now, with the aid of Eq. (A18), we can obtain the e-n structure factor by using either LR or the CCA, i.e., Eq. (11) or Eq. (22) together with Eq. (18). Then, carrying out the numerical integrations with respect to q and λ in Eq. (A5), and using Eq. (A4), we arrive at the total free energy.

[1] See, for example, I.F. Silvera, Rev. Mod. Phys. **52**, 393 (1980); H.K. Mao and R.J. Hemley, *ibid.* **66**, 671 (1994), and references therein.

[2] E. Wigner and H.B. Huntington, J. Chem. Phys. **3**, 764 (1935).

[3] N.W. Ashcroft, Phys. Rev. B **41**, 10 963 (1990); K. Nagao, H. Nagara, and S. Matsubara, *ibid.* **56**, 2295 (1997); K.A. Johnson and N.W. Ashcroft, Nature (London) **403**, 632 (2000); M. Städele and R.M. Martin, Phys. Rev. Lett. **84**, 6070 (2000); T. Takezawa, K. Nagao, and H. Nagara, J. Low Temp. Phys. **123**, 315 (2001).

[4] D.J. Stevenson, Phys. Rev. B **12**, 3999 (1975); W.B. Hubbard and H.E. DeWitt, Astrophys. J. **290**, 388 (1985); H. Kitamura and S. Ichimaru, J. Phys. Soc. Jpn. **67**, 950 (1998).

[5] D. Saumon, G. Chabrier, and H.M. Van Horn, Astrophys. J. **99**, 713 (1995).

[6] L. Cui, N.H. Chen, and I.F. Silvera, Phys. Rev. B **51**, 14 987 (1995); **57**, 656(E) (1998); R.J. Hemley, H.K. Mao, A.F. Goncharov, M. Hanfland, and V. Struzhkin, Phys. Rev. Lett. **76**, 1667 (1996); N.H. Chen, E. Sterer, and I.F. Silvera, *ibid.* **76**, 1663 (1996); P. Loubeyre, R. LeToullec, D. Hausermann, M. Hanfland, R.J. Hemley, H.K. Mao, and L.W. Finger, Nature (London) **383**, 702 (1996); C. Narayana, H. Luo, J. Orloff, and A.L. Ruoff, *ibid.* **393**, 46 (1998); A.F. Goncharov, R.J. Hemley, H.K. Mao, and J. Shu, Phys. Rev. Lett. **80**, 101 (1998).

[7] S.T. Weir, A.C. Mitchell, and W.J. Nellis, Phys. Rev. Lett. **76**, 1860 (1996); W.J. Nellis, S.T. Weir, and A.C. Mitchell, Phys. Rev. B **59**, 3434 (1999).

[8] L.B. Da Silva, P. Celliers, G.W. Collins, K.S. Budil, N.C. Holmes, T.W. Barbee, Jr., B.A. Hammel, J.D. Kilkenny, R.J. Wallace, M. Ross, and R. Cauble, Phys. Rev. Lett. **78**, 483 (1997).

[9] G.W. Collins, L.B. Da Silva, P. Celliers, D.M. Gold, M.E. Foord, R.J. Wallace, A. Ng, S.V. Weber, K.S. Budil, and R. Cauble, Science **281**, 1178 (1998).

[10] A.N. Mostovych Y. Chan, T. Lehecha, A. Schmitt, and J.D. Sethian, Phys. Rev. Lett. **85**, 3870 (2000).

[11] G. I. Kerley, in *Molecular Based Study of Fluids*, edited by J. M. Haile and G. A. Mansoori (ACS, Washington, D.C., 1983), p. 107.

[12] M.W.C. Dharma-wardana and F. Perrot, Phys. Rev. A **26**, 2096 (1982).

[13] F. Perrot, Y. Furutani, and M.W.C. Dharma-wardana, Phys. Rev. A **41**, 1096 (1990).

[14] J. Chihara, Prog. Theor. Phys. **72**, 940 (1984).

[15] T. Kato, Commun. Pure Appl. Math. **10**, 151 (1957).

[16] J.C. Kimball, Phys. Rev. A **7**, 1648 (1973).

[17] A.E. Carlsson and N.W. Ashcroft, Phys. Rev. B **25**, 3474 (1982).

[18] K. Moulopoulos and N.W. Ashcroft, Phys. Rev. B **56**, 4439 (1997).

[19] N.W. Ashcroft and D. Stroud, Solid State Phys. **33**, 1 (1978).

[20] J.-P. Hansen and I. R. McDonald, *Theory of Simple Liquids* (Academic, London, 1976).

[21] B. Militzer and D.M. Ceperley, Phys. Rev. Lett. **85**, 1890 (2000).

[22] A commonly used and equivalent definition of the structure factor is also

$$S_{ij}(q) = \frac{1}{\sqrt{N_i N_j}}\langle \hat{\rho}_i(-\boldsymbol{q})\hat{\rho}_j(\boldsymbol{q})\rangle - \sqrt{N_i N_j}\,\delta_{\boldsymbol{q},0},$$

where $\hat{\rho}_i(\boldsymbol{q}) = \int d\boldsymbol{r}\exp(-i\boldsymbol{q}\cdot\boldsymbol{r})\hat{\rho}_i(\boldsymbol{r})$.

[23] S. Ichimaru, Rev. Mod. Phys. **54**, 1017 (1982).

[24] D. Pines and P. Nozières, *The Theory of Quantum Liquids* (Benjamin, New York, 1966).

[25] U. Gupta and A.K. Rajagopal, Phys. Rep. **87**, 259 (1982).

[26] F. Perrot and M.W.C. Dharma-wardana, Phys. Rev. A **30**, 2619 (1984).

[27] R.G. Dandrea, N.W. Ashcroft, and A.E. Carlsson, Phys. Rev. B **34**, 2097 (1986).

[28] S. Ichimaru, H. Iyetomi, and S. Tanaka, Phys. Rep. **149**, 91 (1987).

[29] Hereafter, the reduced mass μ in Eq. (18) is replaced with the electron mass m_e (adiabatic approximation).

[30] P. Lloyd and C.A. Sholl, J. Phys. C **1**, 1620 (1968); R. Pickenhain, B. Flietner, and K. Unger, Phys. Status Solidi B **154**, 219 (1989).

[31] J. Chihara, J. Phys.: Condens. Matter **3**, 8715 (1991).

[32] J. Chihara, J. Phys. C **19**, 1665 (1986).

[33] S. Tanaka, X.-Z. Yan, and S. Ichimaru, Phys. Rev. A **41**, 5616 (1990).

[34] M.S. Wertheim, Phys. Rev. Lett. **10**, 321 (1963); E. Thiele, J. Chem. Phys. **39**, 474 (1963).

[35] N.F. Carnahan and K.E. Starling, J. Chem. Phys. **51**, 635 (1969); **53**, 600 (1970).

[36] H.D. Jones, J. Chem. Phys. **55**, 2640 (1971).

[37] In the LR approach, the integration with respect to λ is carried out analytically.

[38] However, note that all quantities except the Hugoniot EOS presented in Sec. III are nuclear-mass independent.

[39] G. Galli, R.Q. Hood, A.U. Hazi, and F. Gygi, Phys. Rev. B **61**, 909 (2000).
[40] T.J. Lenosky, S.R. Bickham, J.D. Kress, and L.A. Collins, Phys. Rev. B **61**, 1 (2000).
[41] P. Vashishta and K.S. Singwi, Phys. Rev. B **6**, 875 (1972).
[42] Throughout the calculation, we have set $g_{ee}(0)$ to 0.1, which is a proper value at densities and temperatures where the LFC is significant (see Ref. 23). We also point out that the results presented in this paper are very insensitive to the choice of $g_{ee}(0)$ because $\chi^{(1)}(q)$ at high q is less affected by $G(q)$ (Ref. 27).
[43] R. Abe, Prog. Theor. Phys. **22**, 213 (1959).
[44] W.L. Slattery, G.D. Doolen, and H.E. DeWitt, Phys. Rev. A **21**, 2087 (1980); G.S. Stringfellow, H.E. DeWitt, and W.L. Slattery, *ibid.* **41**, 1105 (1990); H.E. DeWitt and W.L. Slattery, in *Strongly Coupled Coulomb Systems*, edited by G.J. Kalman, J.M. Rommel, and K. Blagoev (Plenum Press, New York, 1998), p. 1, and references therein.
[45] W.R. Magro, B. Militzer, D.M. Ceperley, B. Bernu, and C. Pierleoni, in *Strongly Coupled Coulomb Systems*, edited by G.J. Kalman, J.M. Rommel, and K. Blagoev (Plenum Press, New York, 1998), p. 337.
[46] M. Ross, Phys. Rev. B **58**, 669 (1998); Z. Zinamon and Y. Rosenfeld, Phys. Rev. Lett. **81**, 4668 (1998).